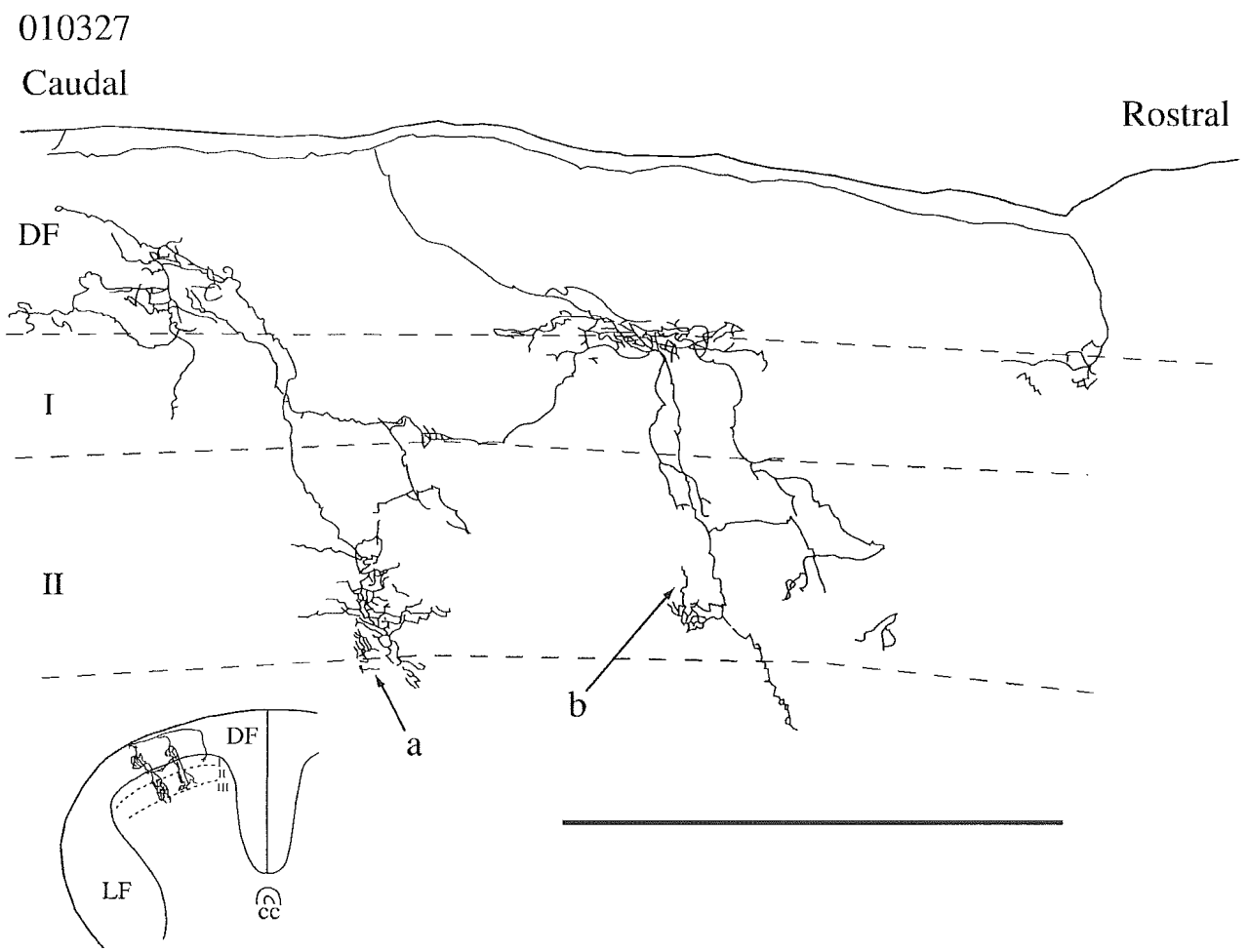

Fig. 3–6. Sagittal views of the reconstructed central projections of C afferent fibers from the lateral gastrocnemius (LGC) muscle labeled with *Phaseolus vulgaris*-leucoagglutinin (PHA-L) in the L5 dorsal root ganglion. The axon ran rostrally along the dorsal surface of the spinal cord, then issued a few collaterals to laminae I, II, and III. Solid and open stars, rhombuses, and number signs indicate the interrupted drawings. Broken lines indicate borders of laminae I, II, and III. The figure in the **insets** was a superimposed feature of the same fiber in the transverse plane. Transverse drawings showed relative locations of the central arbors of C fiber terminals in laminae of the dorsal horn. CC, central canal; LF, lateral funiculus; DF, dorsal funiculus. Scale bars = 500 μm.

Fig. 3. Sagittal view of reconstructed fiber No. 010327. The main axon issued collaterals to make a few restricted terminal distributions in laminae I and II and DF. Arrows a and b indicate the branches that are drawn at high magnification in Figure 7a,b. Terminal areas were located in laminae II and III, in which terminal swellings produced a densely compacted terminal field.

The central collaterals and branches of the LGC muscle C fibers in the superficial dorsal horn of the lumbar cord were very thin. Sometimes we observed, at lower than light microscopic resolution, extremely thin fibers between terminal swellings in the terminal plexuses of LGC muscle C fibers. The arbors of well-labeled fibers could generally be traced up to terminal enlargements in the entry segment of the root (Fig. 2a,b); some fiber terminals were traced in several segments regardless of faint staining or interruption of fiber trajectories in the dorsal funiculus and superficial dorsal horn (Fig. 2c,d).

Spinal distribution of central terminals of C muscle afferent fibers

From the sagittal view of one reconstructed fiber (No. 010327), we determined that the axon-issued collaterals distributed a few, small, circumscribed groups of terminals in lamina I, lamina II, and dorsal funiculus (DF). Moreover, some terminal collaterals extended to the border of lamina III (Fig. 3); here, the terminal areas extended 100–200 μm rostrocaudally. From light micrographs, we observed that the labeled fiber distributed among the DF and lamina I and showed terminal swellings (Fig. 2a,b); the terminals in lamina II were small, complex, and densely packed (Figs. 3a,b, arrows, 7a,b). The distribution pattern of the densely packed terminal swellings on this fiber was slightly different from the patterns of other fibers (Fig. 7).

The fiber with C fiber latency (No. 010403) showed terminal areas forming a nest-like field in the DF and at the border of laminae I and II and middle lamina II. Two major terminal plexuses, which showed relatively sparse

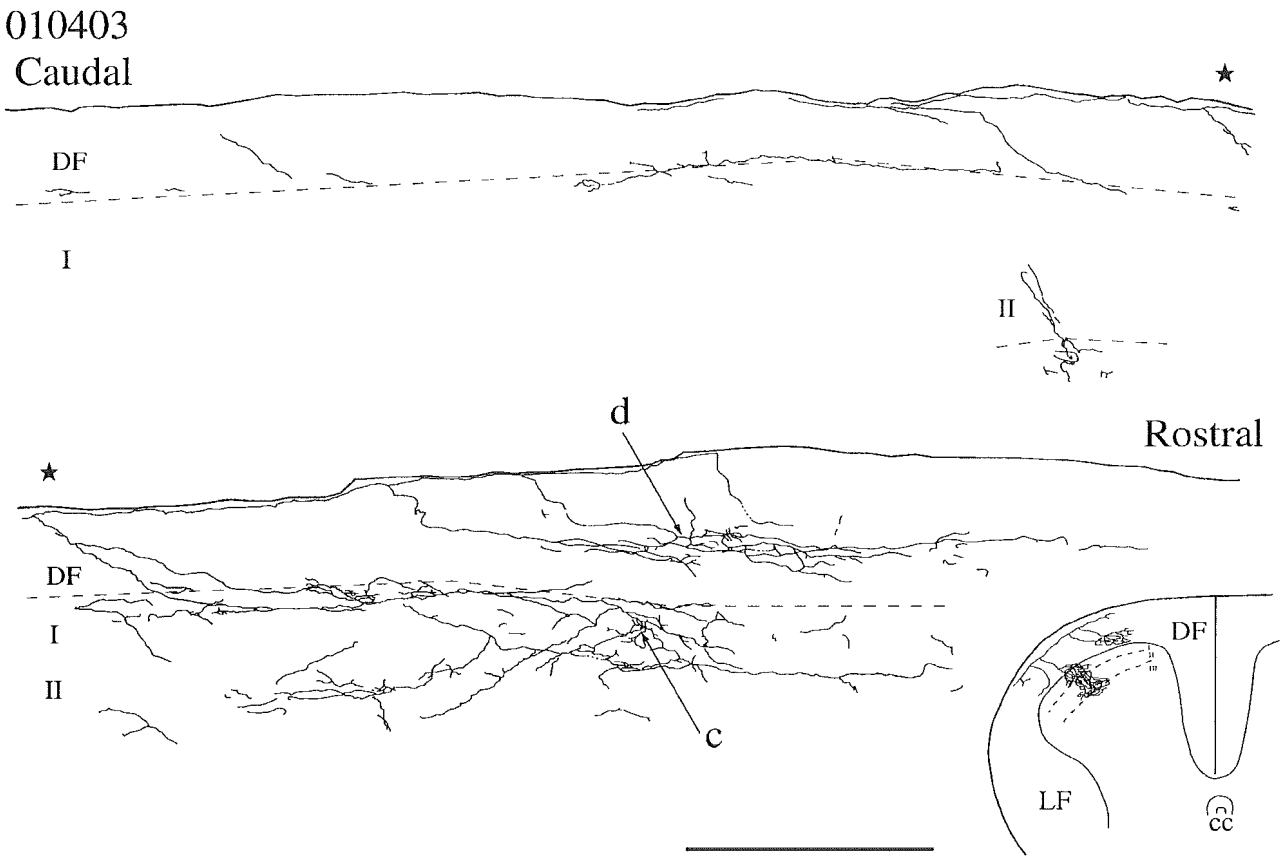

Fig. 4. Sagittal view of labeled fiber No. 010403, which terminated between the DF and lamina I. Fiber terminals exhibited a sparsely distributed, nonconcentrated terminal focus in DF, lamina I, and lamina II, connecting with very fine fibers between each terminal area. Terminal field extended about 700μm rostrocaudally. Arrows c and d indicate branches depicted in Figure 7c and d, respectively.

and faintly stained terminal arbors (Fig. 2c), connected with the very fine fibers and thin, small terminals extending about 700 μm rostrocaudally (Fig. 4). Total termination areas extended about 1 mm in the spinal cord, connecting with the very fine fibers from this particular fiber. The terminal plexuses were composed of terminal branches and swellings with fairly straight arrays and forms (Figs. 4c,d, arrows, 7c,d).

A sagittal view of another reconstructed fiber (No. 010206) showed some concentrated terminal regions distributed over 500 μm rostrocaudally in laminae I and II (Fig. 5). The terminal plexuses showed complex terminal branches, which were sharply demarcated areas and had relatively small terminal swellings (Figs. 4e,f, arrows, 7e,f).

In animal 010201, the fiber axon ran along the surface of the DF, then issued collaterals to laminae I and II and the DF. The sagittal drawing of this C fiber revealed that it extended almost 1 cm rostrocaudally and gave off several collaterals from the main branches running along the DF and terminating in three terminal areas in laminae I and II; some collaterals also terminated in the DF. Their branches showed a simple, straight arrangement of terminal swellings (Figs. 6g,h, arrows, 7g,h).

In short, the LGC muscle C afferents, which were not identified for their receptor modality, projected to the dorsal spinal cord rostrocaudally over several segments and ran along the surface of the DF, giving off collaterals to laminae I and II and at the border of lamina III. Terminal branches of C fibers were found not only in the gray matter of the superficial dorsal horn but also in the DF around the dorsal horn. The terminal branches, however, were not densely enough concentrated to form the remarkably circumscribed terminal plexuses of the cutaneous C afferent fibers observed in previous studies (Sugiura et al., 1989, 1993). Furthermore, a muscle C afferent fiber had two or three terminal regions distributed over the rostrocaudal length of the two or three spinal segments.

Number and size of terminal swellings

The numbers of terminal boutons found in LGC muscle C or group IV fibers in this study are summarized in Table 1. Some 3,500–5,000 enlargements (boutons) were identified on each fiber, almost all of which were found in the superficial dorsal horn (laminae I and II), in the DF, and occasionally in lamina III. Consequently, we found that one terminal plexus of identified muscle C fiber had

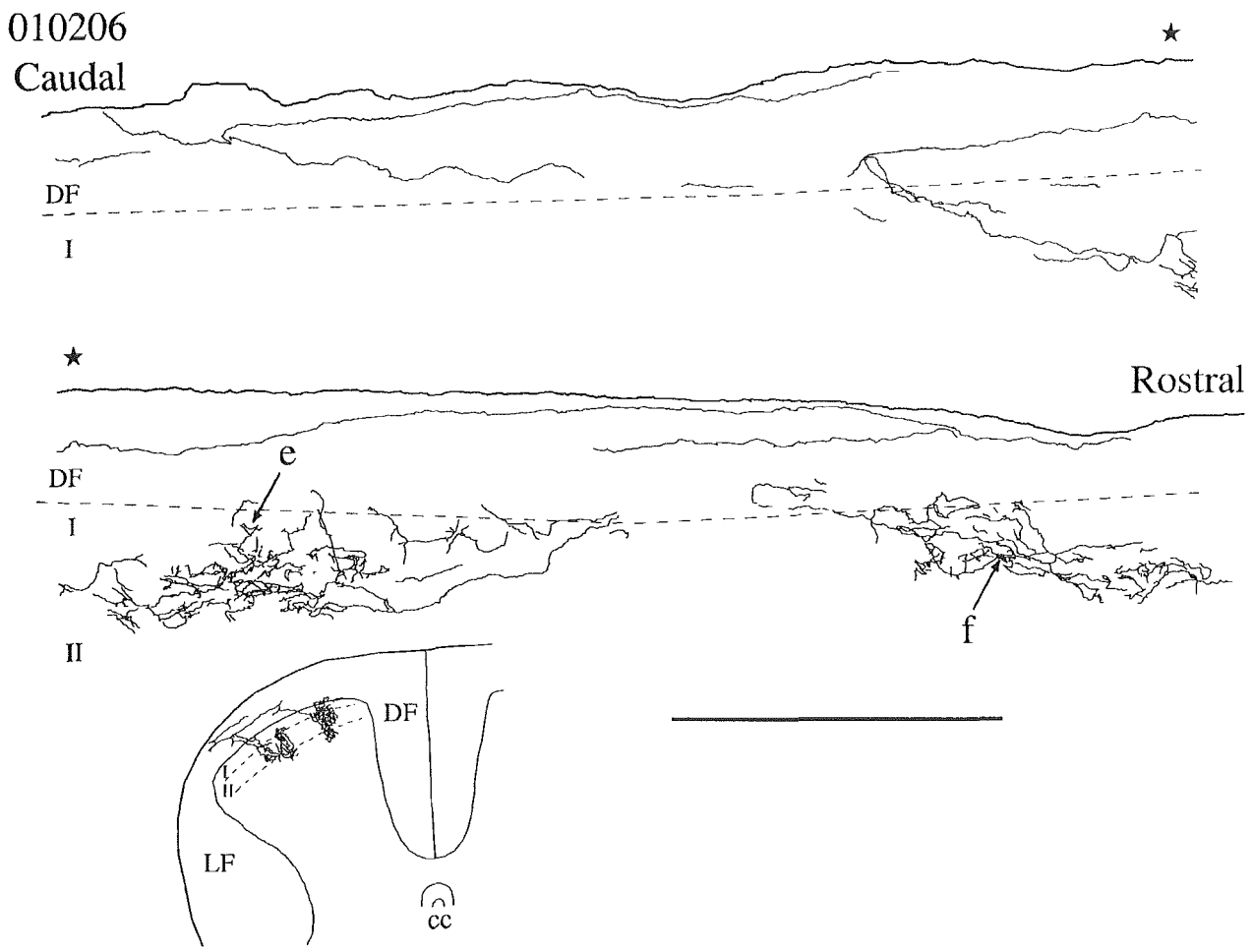

Fig. 5. Sagittal view of reconstructed fiber No. 010206. This fiber exhibited two concentrated terminal regions distributed over 500 μm in rostrocaudal length. Arrows e and f indicate the branches shown in Figure 7e and f, respectively.

1,500–2,000 terminal boutons or synaptic swellings in each terminal area.

In the DF, terminal swellings were fairly flat, and their diameters reached almost 5–6 μm, whereas those in lamina II were relatively round and smaller than 3.5 μm. The sizes of terminal swellings in lamina I are distributed between those found in the DF and those found in lamina II (Fig. 8).

DISCUSSION

This study is, to our knowledge, the first report to demonstrate the central projections of unmyelinated C and group IV muscle afferent fibers. Our results reveal the whole central trajectories of C afferent fibers from the LGC muscle; these fibers terminate mainly in the DF and superficial dorsal horn (laminae I and II).

Technical considerations

This study was hampered by the fact that the number of observed C fibers was limited in spite of a large number of labeled ganglion cells. Although good unitary responses from C afferent neurons in DRGs were recorded over a sufficient period, the sufficient current passage for iontophoresis with PHA-L often resulted in the disappearance of neuronal activity in spite of proper maintenance of intracellular voltage. Furthermore, even if the recording of unitary responses and labeling of DRG cells appeared to be maximal, we found in some preparations that the PHA-L concentration was not enough to label the terminations of central branches and to permit tracing of fiber branches. Consequently, only about 15% of the unmyelinated muscle fibers could be recovered; for those, however, nearly all the full trajectories from labeled or definite unmyelinated cells were traced.

Although we could not characterize the responses of the C fibers to natural stimuli because of the difficulty of keeping the intracellular recording stable for sufficient time, we believe that these fibers may innervate vessels, muscle capsules, and deep connective tissues in the LGC. Because we could not evoke impulses from the muscle, stimuli other than strong mechanical activation applied through the skin may have been required to activate the

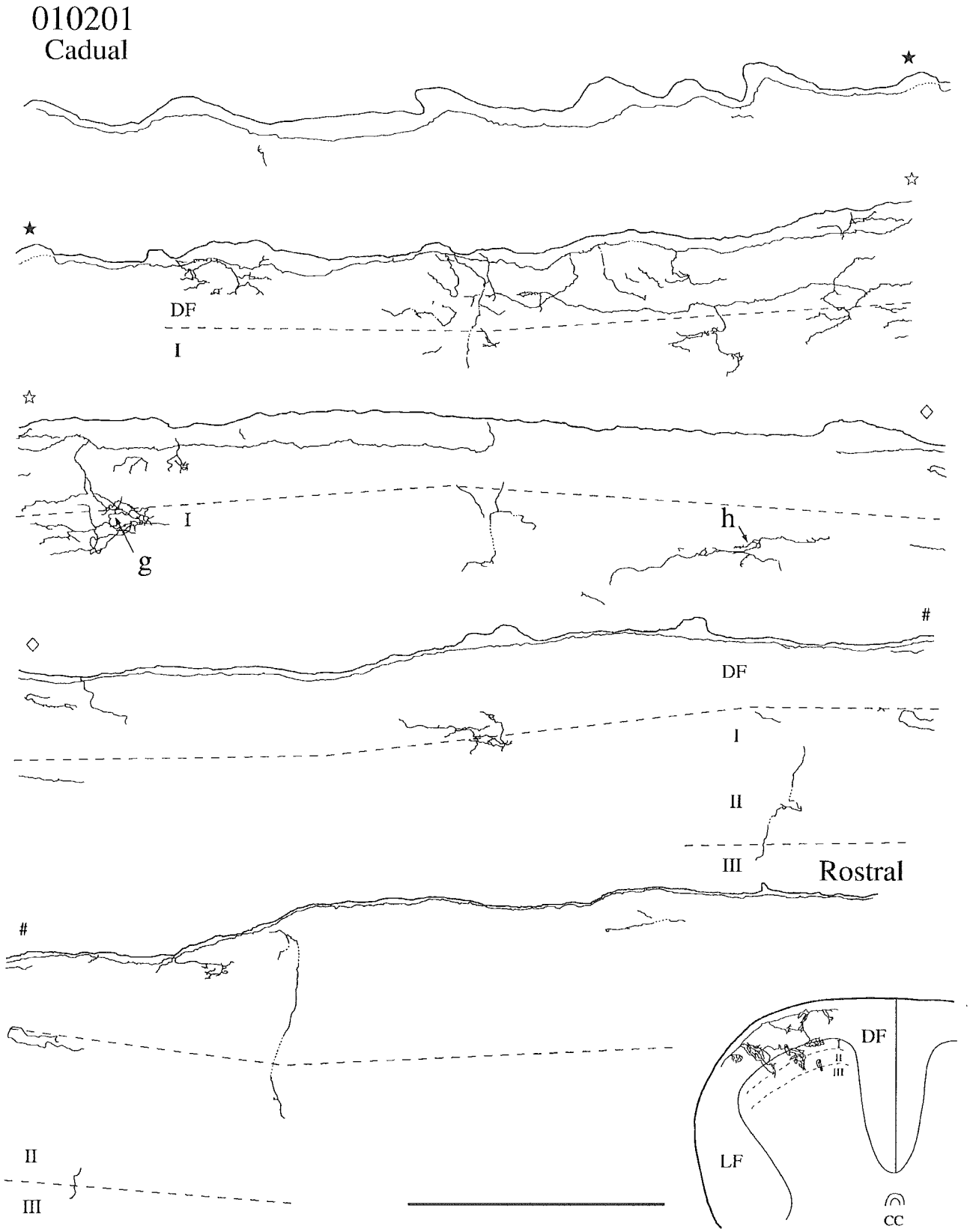

Fig. 6. Sagittal drawing of C afferent fiber No. 010201, which extended almost 1 cm rostrocaudally. About five collaterals left the main branches to terminate in laminae I and II, and some collaterals also terminated in the dorsal funiculus. Some terminal branches could not be traced from the main axon running along the DF, because fibers were under light microscopic resolution or faintly stained. Arrows g and h indicate the branches depicted in Figure 7g and h, respectively.

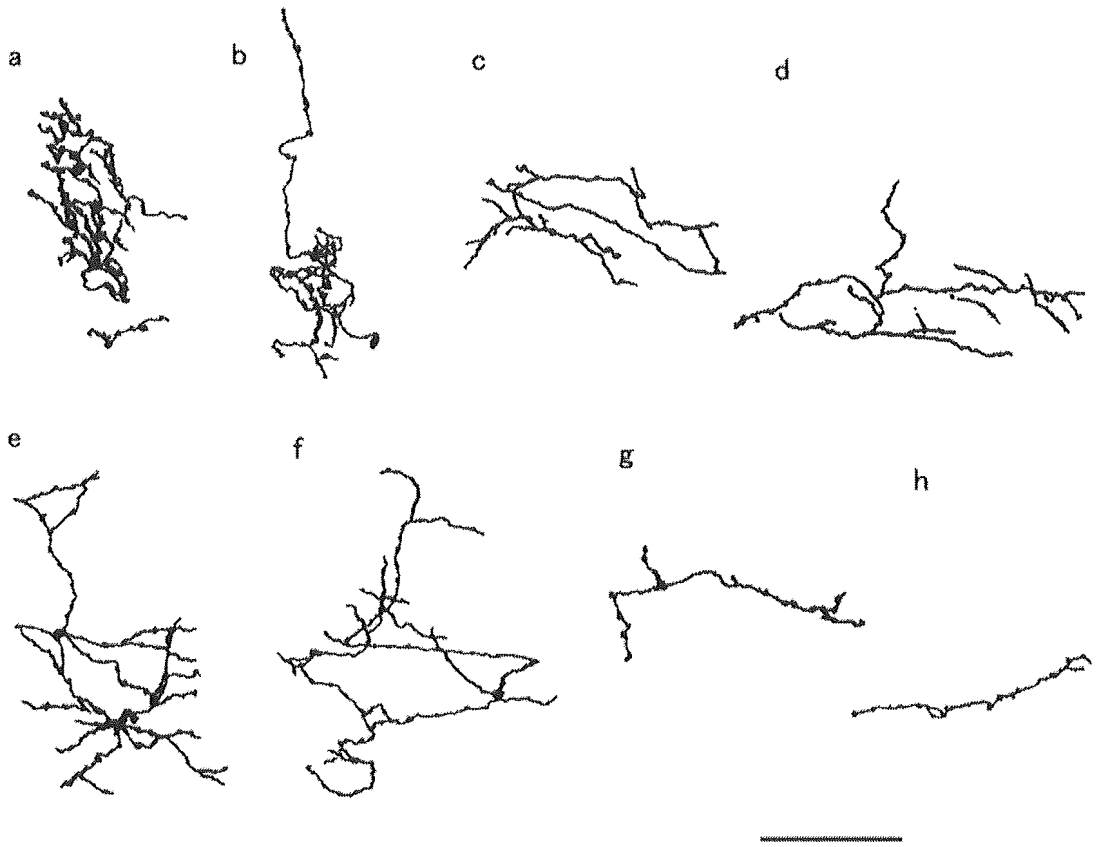

Fig. 7. Two branches selected from each muscle afferent C fiber shown in Figures 3–6. Arrows a–h at branches in Figures 3–6 correspond to the respective Figure 7a–h drawn at high magnification. Terminal branches of 7a and 7b, which had densely packed terminal branches in each terminal area, appeared slightly different from the other terminals. The array of each terminal branch was basically arranged with the orientation of the neuropil of the laminae in the dorsal horn. Scale bar = 50 μm.

TABLE 1. Numbers of Terminal Boutons

	Animal No.			
	010201	010206	010327	010403
No. of boutons	4,670	3,463	4,714	3,803
DF	3,261	1,068	1,660	841
Laminae I and II	1,393	2,395	2,874	2,927
Lamina III	16		180	35
No. of areas	3	2	3	2

receptors (Kumazawa and Mizumura, 1977; Mense and Meyer, 1985).

Differential termination of muscle afferent fibers

Several investigators have described the central projections of myelinated afferent fibers of muscle: Large-diameter afferent fibers terminate in laminae IV, V, and VI and in the interneuron and motoneuron pools of laminae VII and IX (Brown and Fyffe, 1977, 1979; Ishizuka et al., 1979); thinly myelinated and small-diameter afferent fibers from muscle send terminals to laminae I and V (Réthelyi et al., 1982; Craig and Mense, 1983; Nyberg and Blomqvist, 1984; Mense and Craig, 1988).

Previous studies used antidromic microstimulation to show that terminal arborizations of unmyelinated muscle afferent fibers could extend into deep lamina II (MacMahon and Wall, 1985). Hoheisel and Mense (1990) also showed that neurons in lamina I and V responded to stimulation of C fiber muscle nerve fibers. Application of horseradish peroxidase or the cholera toxin B subunit to the muscle labeled structures, including central terminals of C muscle afferent fibers in the superficial dorsal horn and lamina II over several time courses (Ygge, 1989; Hirakawa et al., 1992). Capsaicin-sensitive muscle afferent fibers, which may have C or unmyelinated fibers, terminated in laminae I and II (Torre et al., 1995).

Previous studies have shown that cutaneous C fibers terminated principally in laminae I and II of the dorsal horn; moreover, they terminated in circumscribed and concentrated zones containing many enlargements and synaptic boutons (Sugiura et al., 1986, 1989). Unlike cutaneous C fibers, which have a concentrated terminal focus, visceral afferent C fibers typically have only one or two terminal branches at each terminal locus within several enlargements. C fibers of visceral origin terminated ipsilaterally in laminae I, II, V, and X, and some fibers projected contralaterally to laminae V and X (Sugiura et al., 1989).

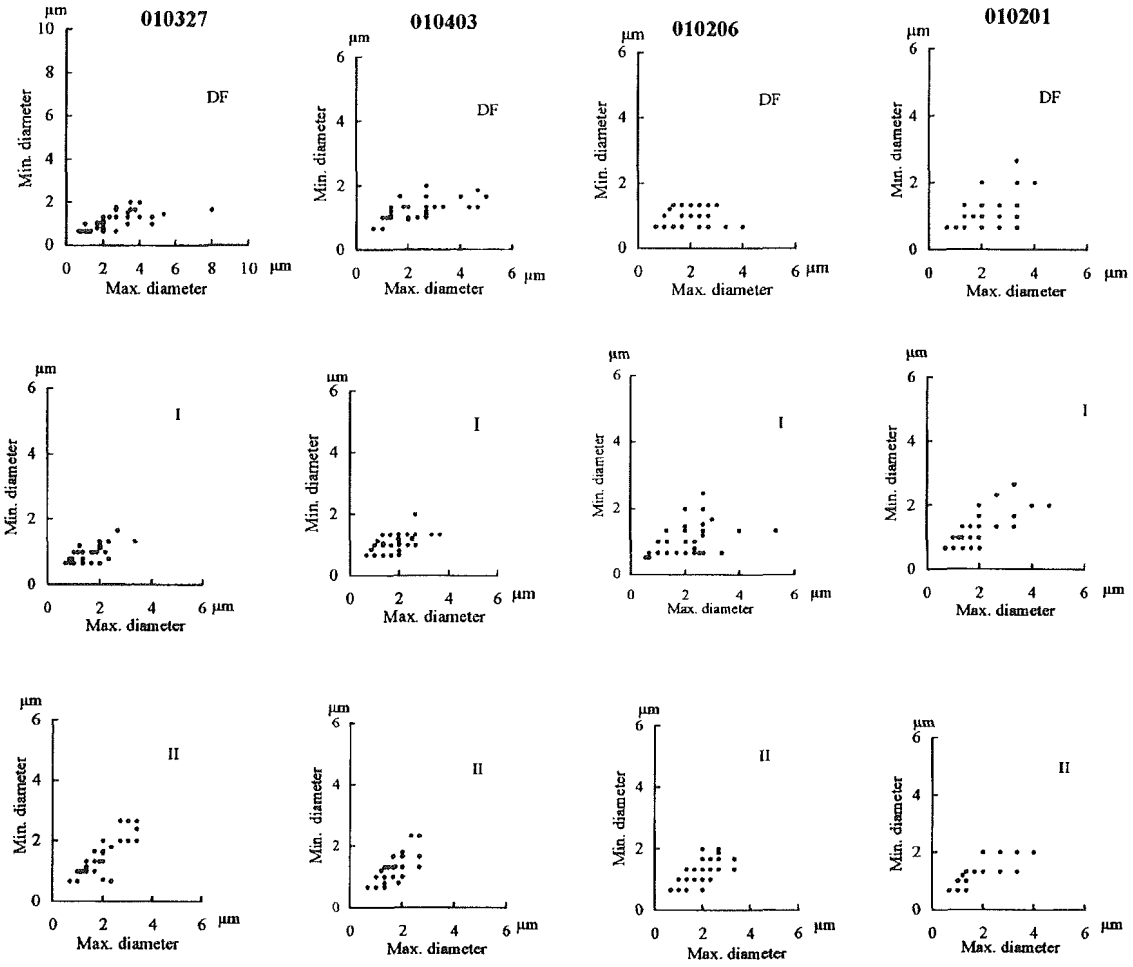

Fig. 8. Size distribution of terminal swellings in the dorsal horn. Fifty terminal swellings were measured in the DF, lamina I (I), and lamina II (II). Terminal swellings in lamina II were almost round and were under 3.5 μm in diameter. Fiber swellings in DF were relatively flat, and few reach 8 μm. Terminal swellings in lamina I were smaller than 3.5 μm, reflecting their intermediate size between those in lamina II and DF.

LGC muscle C afferents projected rostrocaudally over several segments, running on the surface of the DF and giving off collaterals ipsilaterally to laminae I and II and partly to lamina III. Most of the terminal arbors and boutons were localized in laminae I and II and the DF. From the results regarding muscle terminals, we conclude that these terminal locations are similar to that of cutaneous C afferent fibers but that the distribution of the terminal plexuses is different from the distributions of cutaneous and visceral C afferent fibers. C fibers from muscle coursed through the DF (and not through Lissauer's tract, as previously believed), with collaterals emanating over three segments and more, exhibiting a substantial termination in the white matter dorsal to lamina I. These fibers could provide inputs to the poorly defined neurons occasionally reported for the DF (Mizumura et al., 1993; Sugiura et al., 1993).

In summary, we found terminations of muscle C afferent fibers in lamina II as well as in lamina I. Lamina II neurons rarely have been tested for inputs from muscle. Interestingly, several of the fibers seemed to have a "dual" termination pattern, with many endings in lamina I and many more deeper in lamina II.

Number and size of terminal swellings

The number of muscle C fiber terminal swellings in a single zone was smilar to that of cutaneous C fibers, but the terminal fields of the former extended two or three times more three-dimensionally (dorsoventrally, mediolaterally, and rostrocaudally) than those of the latter. Moreover, the terminal swellings of muscle afferent were relatively less densely clustered than those of cutaneous C fibers. The density of terminations from muscle afferent was found to be intermediate between those of cutaneous

C fibers and visceral C afferents. The forms of the terminal plexus and the complexity of the terminal array in the LGC muscle C afferent fiber projection were fairly different from those of the cutaneous and visceral C fibers (Sugiura et al., 1993). The synaptic terminals or terminal swellings of the LGC muscle C afferents were small and relatively round in laminae I and II. The size and irregularity of terminal swellings of these muscle C fibers (<3.5 μm) ranged between those of cutaneous (1–5 μm) and visceral (<3 μm) terminals and might belong to a smaller group, closer in size to visceral terminals. The size distribution of terminal swellings in muscle afferents is reported to be similar to the terminal profile of capsaicin-sensitive muscle afferent fibers, which have small, nonscalloped synapses (Torre et al., 1995), and to visceral C afferent terminals, having small, round, central synapses (Sugiura and Tonosaki, 1995). These profiles are different from cutaneous C afferent terminals, which possess large, central glomeruli and scalloped synapses.

Functional considerations

In muscle, thick, myelinated afferent fibers transmit a proprioceptive input used for detecting muscle tonus, stretch, and contraction. Group III, group IV, and C fibers may transmit a certain sensory modality, especially pain, as do cutaneous and visceral afferent fibers. Fibers relating to pain distribute in the fascia and connective tissues among the muscle fibers and respond to mechanical and noxious stimuli. Signals occurring in deep pressure or pain stimuli in the muscle are transmitted to the superficial spinal cord.

Nociceptive information from muscle pain does not detail a clear somatotopic arrangement depending on the locality of the fascia and muscle capsules. The central projections of muscle C or group IV fibers into the spinal cord spread beyond several spinal segments, reflecting spreading pain sensation. Our observations demonstrate that the central projections of muscle C afferent fibers characteristically transmit pain and other sensations from muscle organs with more somatotopic sharpness than do visceral afferents, but this is more vague and more widespread than that with cutaneous afferents.

ACKNOWLEDGMENTS

We thank Dr. Alan Light and Ms. Bonnie Blake for scientific comments and for help with the English.

LITERATURE CITED

Abraham VC, Swett JE. 1986. The pattern of spinal and medullary projections from a cutaneous nerve and muscle nerve of the forelimb of the cat: a study using the transganglionic transport of HRP. J Comp Neurol 246:70–84.

Abraham VC, Richmond FJ, Keane J. 1984. Projections from C2 and C3 nerves supplying muscle and skin of the cat neck: a study using transganglionic transport of horseradish peroxidase. J Comp Neurol 230: 142–154.

Alvarez FJ, Kavookjian AM, Light AR. 1993. Ultrastructural morphology, synaptic relationships, and CGRP immunoreactivitiy of physiologically identified C-fiber terminals in the monkey spinal cord. J Comp Neurol 329:472–490.

Arvidsson J, Pfaller K. 1990. Central projections of C4–C8 dorsal root ganglia in the rat studied by anterograde transport of WGA-HRP. J Comp Neurol 292:349–362.

Arvidsson J, Rice FL. 1991. Central projections of primary sensory neurons innervating different parts of the vibrissae follicles and intervibrissal skin on the mystacial pad of the rat. J Comp Neurol 309:1–16.

Brown AG. 1981. Organization in the spinal cord. The anatomy and physiology of identified neurons. New York: Springer-Verlag. p 1–238.

Brown AG, Fyffe REW. 1977. The morphology of group Ia afferent fiber collaterals in the spinal cord of the cat. J Physiol 274:111–127.

Brown AG, Fyffe REW. 1979. The morphology of group Ib afferent fiber collaterals in the spinal cord of the cat. J Physiol 296:215–228.

Brown AG, Rose PK, Snow PJ. 1978. Morphology and organization of axon collaterals from afferent fibres of slowly adapting type I units in cat spinal cord. J Physiol 277:15–27.

Brown AG, Fyffe REW, Noble R. 1980. Projections from pacinian corpuscles and rapidly adapting mechanoreceptors of glabrous skin to the cat's spinal cord. J Physiol 307:385–400.

Brown PB, Gladfelter WE, Culberson JC, Covalt-Dunning D, Sonty RV, Pubols LM, Millecchia RJ. 1991. Somatotopic organization of single primary afferent axon projections to cat spinal cord dorsal horn. J Neurosci 11:298–309.

Brushart TM, Henry EW, Mesulam M-M. 1981. Reorganization of muscle afferent projection accompanies peripheral nerve regeneration. Neuroscience 6:2053–2061.

Capra NF, Wax TD. 1989. Distribution and central projections of primary afferent neurons that innervate the masseter muscle and mandibular periodontium: a double-label study. J Comp Neurol 279:341–352.

Carson KA, Mesulam M-M. 1982. Ultrastructural evidence in mice that transganglionically transported horseradish peroxidase-wheat germ agglutinin conjugate reaches the intraspinal terminations of sensory neurons. Neurosci Lett 29:201–206.

Castro-Lopes JM, Coimbra A. 1991. Spinal cord projections of the rat main forelimb nerves, studies by transganglionic transport of WGA-HRP and by the disappearance of acid phosphatase. Brain Res 542:187–192.

Cervero F, Connell LA. 1984. Distribution of somatic and visceral primary afferent fibers within the thoracic spinal cord of the cat. J Comp Neurol 230:88–98.

Craig AD, Mense S. 1983. The distribution of afferent fibers from the gastrocnemius-soleus muscle in the dorsal horn of the cat, as revealed by the transport of horseradish peroxidase. Neurosci Lett 41:233–238.

Fyffe REW. 1984. Afferent fibers. In: Davidoff RA, editor. Handbook of the spinal cord. New York: Marcel Dekker. p 79–136.

Gerfen CR, Sawchenko PE. 1984. An anterograde neuroanatomical tracing method that shows the detailed morphology of neurons, their axons and terminals: immunohistochemical localization of an axonally transported plant lectin, phaseolus vulgaris leucoagglutinin (PHA-L). Brain Res 290:219–238.

Gobel S, Fall WM, Humphrey E. 1981. Morphology and synaptic connections of ultrafine primary axon in lamina I of the spinal dorsal horn: candidates for the terminal axonal arbors of primary neurons with unmyelinated (C) axons. J Neurosci 1:1163–1179.

Hirakawa M, McCabe JT, Kawata M. 1992. Time-related changes in the labeling pattern of motor and sensory neurons innervating the gastrocnemius muscle, as revealed by the retrograde transport of the cholera toxin B subunit. Cell Tissue Res 267:419–427.

Hoheisel U, Mense S. 1990. Response behaviour of cat dorsal horn neurons receiving input from skeletal muscle and other deep somatic tissues. J Physiol 426:265–280.

Hoheisel U, Lehmann-Willenbrock E, Mense S. 1989. Termination patterns of identified group II and III afferent fibres from deep tissues in the spinal cord of the cat. Neuroscience 28:495–507.

Hongo T, Kudo N, Sasaki S, Yamashita M, Yoshida K, Ishizuka N, Mannen H. 1987. Trajectory of group Ia and Ib fibers from the hind-limb muscle at the L3 and L4 segments of the spinal cord of the cat. J Comp Neurol 262:159–194.

Ishizuka N, Mannen H, Hongo T, Sasaki S. 1979. Trajectory of group Ia afferent fibers stained with horseradish peroxidase in the lumbosacral spinal cord of the cat: three dimensional reconstructions from serial sections. J Comp Neurol 186:189–212.

Kalia M, Mei SS, Kao FF. 1981. Central projections from ergoreceptors (C fibers) in muscle involved in cardiopulmonary responses to static exercise. Circ Res 48:48–62.

Kumazawa T, Mizumura K. 1977. Thin fibre receptors responding to mechanical, chemical and thermal stimulation in the skeletal muscle of the dog. J Physiol 273:179–194.

Light AR, Perl ER. 1979a. Reexamination of the dorsal root projection to the spinal dorsal horn including observations on the differential termination of coarse and fine fibers. J Comp Neurol 186:117–132.

Light AR, Perl ER. 1979b. Spinal termination of functionally identified primary afferent neurons with slowly conducting myelinated fibers. J Comp Neurol 186:133–150.

McMahon SB, Wall PD. 1985. The distribution and central termination of single cutaneous and muscle unmyelinated fibers in rat spinal cord. Brain Res 359:39–48.

Mense S. 1993. Nociception from skeletal muscle in relation to clinical muscle pain. Pain 54:241–289.

Mense S, Craig AD. 1988. Spinal and supraspinal terminations of primary afferent fibers from the gastrocnemius-soleus muscle in the cat. Neuroscience 26:1023–1035.

Mense S, Meyer H. 1985. Different types of slowly conducting afferent units in cat skeletal muscle and tendon. J Physiol 363:403–417.

Mense S, Prabhakar NR. 1986. Spinal termination of nociceptive afferent fibres from deep tissues in the cat. Neurosci Lett 66:169–174.

Mense S, Light AR, Perl ER. 1981. Spinal terminations of subcutaneous high-threshold mechanoreceptors. In: Brown AG, Réthelyi M, editors. Spinal cord sensation. Edinburgh: Scottish Academic Press. p 79–86.

Mizumura K, Sugiura Y, Kumazawa T. 1993. Spinal termination patterns of canine identified A and C spermatic polymodal receptors traced by intracellular labeling with *Phaseolus vulgaris*-leucoagglutinnin. J Comp Neurol 335:460–468.

Nyberg G, Blomqvist A. 1984. The central projection of muscle afferent fibers to the lower medulla and upper spinal cord: an anatomical study in the cat with the transganglionic transport method. J Comp Neurol 230:99–109.

Pfaller K, Arvidsson J. 1988. Central distribution of trigeminal and upper cervical primary afferents in the rat studied by anterograde transport of horseradish peroxidase conjugated to wheat germ agglutinin. J Comp Neurol 268:91–108.

Prihoda M, Hiller M-S, Mayr R. 1991. Central projections of cervical primary afferent fibers in the guinea pig: an HRP and WGA/HRP tracer study. J Comp Neurol 308:418–431.

Réthelyi M, Capowski JJ. 1977. The terminal arborization pattern of primary afferent fibers in the substantia gelatinosa of the spinal cord in the cat. J Physiol 73:269–277.

Réthelyi M, Light AR, Perl ER. 1982. Synaptic complexes formed by functionally defined primary afferent units with fine myelinated fibers. J Comp Neurol 207:381–393.

Snow PJ, Rose PK, Brown AG. 1976. Tracing axons and axon collaterals of spinal neurons using intracellular injection of horseradish peroxidase. Science 191:312–313.

Sugiura Y, Tonosaki Y. 1995. Spinal organization of unmyelinated visceral afferent fibers in comparison with somatic afferent fibers. In: Gebhart GF, editor. Visceral pain. Progress in pain research and management, vol 5. Seattle: IASP Press.

Sugiura Y, Lee CL, Perl ER. 1986. Central projections of identified, unmyelinated (C) afferent fibers innervating mammalian skin. Science 234: 358–361.

Sugiura Y, Terui N, Hosoya Y. 1989. Difference in distribution of central terminals between visceral and somatic unmyelinated (C) primary afferent fibers. J Neurophysiol 62:834–840.

Sugiura Y, Terui N, Hosoya Y, Tonosaki Y, Nishiyama K, Honda T. 1993. Quantitative analysis of central terminal projections of visceral and somatic unmyelinated (C) primary afferent fibers in the guinea pig. J Comp Neurol 332:315–325.

TerHorst GJ, Groenwegen HJ, Karust H, Luiten PGM. 1985. *Phaseolus vulgaris* leucoagglutin immunocytochemistry. A comparison between autoradiographic and lectin tracing neuronal efferents. Brain Res 307: 379–383.

Torre GD, Lucchi ML, Burnetti O, Pettorssi VE, Clavenzani P, Bortolami R. 1995. Central projection and entries of capsaicin-sensitive muscle afferents. Brain Res 713:223–231.

Ygge J. 1989. Central projection of the rat radial nerve investigated with transganglionic degeneration and transganglionic transport of horseradish peroxidase. J Comp Neurol 279:199–211.

Ygge J, Grant G. 1983. The organization of the thoracic spinal nerve projection in the rat dorsal horn demonstrated with transganglionic transport of horseradish peroxidase. J Comp Neurol 216:1–9.

Environmental Medicine, 47, 2003 (page 26 ~ 30)

A Trial to Evaluate Experimentally Induced Delayed Onset Muscle Soreness and Its Modulation by Vibration

Tomoko KOEDA,[1,2] Takahiro ANDO,[2] Takayuki INOUE,[2] Kenta KAMISAKA,[2] Shinya TSUKAMOTO[2]
Takahiro TORIKAWA,[2] Jun HIRASAWA,[2] Makoto YAMAZAKI,[2] Kunio IDA[2] and Kazue MIZUMURA[1]
[1] Department of Neural Regulation
Division of Regulation of Organ Function
Research Institute of Environmental Medicine
Nagoya University, Nagoya 464-8601, Japan
[2] Department of Physical Therapy
School of Health Sciences
Nagoya University, Nagoya 461-8673, Japan

Abstract: Clinical muscular pain such as stiff neck and lumbago is often treated with massage, stretch, and vibration; however, the effectiveness of these procedures and their action mechanisms remain unclear. We consider it important to quantitatively evaluate the effectiveness of these procedures using experimentally induced muscular pain. Exercise-induced pain has been used as a model of muscular pain. In the present experiment, we used this model to evaluate the effect of vibration, which is used in physical therapy. Muscle soreness was induced by exercise of the upper arm using a weight belt, and changes in the muscle were evaluated using limb circumference, joint angle, strength of muscle soreness, dimensions of muscle and blood flow before and after exercise and vibration. The present exercise protocol induced delayed onset muscle soreness 1 day after exercise. Vibration given immediately and 2 days after exercise widened the limited range of motion, decreased muscle soreness in full flexion and extension positions, increased blood flow in the deep tissues involving muscle and another connective tissues, increased the thickness of subcutaneous tissues, and tended to decrease the thickness of flexors. However, in contrast to our clinical experience, these effects did not last long after vibration. The reason for this might be that the kind of pain was different.

Key words: delayed onset muscle soreness, vibration, human, muscle evaluation

The mechanisms of clinical muscular pain such as stiff neck and lumbago remain insufficiently understood, although this kind of pain is often a chief complaint of patients visiting clinics or hospitals. The affected muscles often have trigger points with locally contracted muscle fibers. Massage and stretch are often used by physical therapists to stretch and relax the shortened or stiff muscle and to relieve pain. However, the effectiveness of these procedures and their action mechanisms are unclear. We consider it important to quantitatively evaluate the effectiveness of these techniques using experimentally induced muscular pain. One such model that has been used in humans and animals is exercise-induced pain. Delayed onset muscle soreness (DOMS) usually occurs 24 to 48 hours after unaccustomed exercise (Smith 1991), especially after eccentric exercise. Such exercise damages the muscle and another connective tissue, and has been shown subsequently to cause inflammatory responses (Armstrong, Warren et al. 1991). However, Nosaka and Clarkson (1996) claimed that the inflammatory responses such as muscle swelling and soreness after exercise were different from those accompanying infection or tissue injury, because none of the plasma levels of inflammatory markers showed significant changes after exercise. Although there is some controversy regarding the mechanism for development of DOMS, as described above, it can be consistently produced; thus, we consider it useful for evaluating the effect of physical therapy. In this experiment we attempted to develop a DOMS model using a weight belt, which is easy to handle and can be used anywhere, and evaluated muscle condition from many aspects. Next, we evaluated the effect of vibration stimulation, which has recently been used for treatment of muscular pain, on changes in the affected muscle. Vibration stimulation was used instead of massage because vibration at low frequency has some common features with massage, and is considered to be more easily quantified than massage done with the hands.

Material and methods

Subject and experimental protocol

The subjects were 24 healthy volunteers (12 males and 12 females), with ages ranging from 19 to 23 years (mean 20.8 years). Each subject gave informed consent. They were ran-

Reprint requests to: Dr. Kazue MIZUMURA at above address.
This work was partly supported by a Health and Labour Sciences Research Grant from the Ministry of Health, Labour and Welfare (H14-Choju-29).

domly assigned to one of three groups, with the sex ratio kept the same in each group: control group (exercise only), vibration immediately after exercise (early-V group), and vibration 2 days after exercise (late-V group). The subjects lay supine, and a load was placed on the wrist of their non-dominant arm. The weight was adjusted according to the subject's sex (2 kg for women and 3 kg for men). With the weight wrapped around their non-dominant arm, the subjects were instructed to lower the arm from a position of 60 degree to 20 degree elbow flexion over 5 sec, and then to return it to the initial 60 degree flexion position over another 5 sec. This exercise was continued until exhaustion (the subject could no longer perform the movements), and 3 sets with the same load were done with a 5 min rest period between sets. Starting from the 2nd set, when a subject was unable to flex the elbow joint by him- or herself, the experimenter manually assisted the subject in bringing the arm to the flexed position.

Measurement

All subjects underwent the following measurements to evaluate changes in the muscle condition: circumference of the upper arm, range of motion (ROM; arm angles in both directions at elbow joint), muscle perception (soreness and dull sensation), blood flow in deep tissues, and ultrasound images of the muscle. These were measured before and immediately after the exercise, and 2 and 7 days after the exercise. They were also measured after vibration in the two vibration groups. All parameters except muscle perception were measured three times at each time point and data thus obtained were averaged. The circumference of the upper arm was measured at a point approximately one-third of the upper arm length distal from the epicondyle of the humerus, which was marked with a felt-tipped pen. ROM at the elbow joint was measured using a goniometer in flexion and extension. Soreness and dull sensation in the muscle were assessed using a numerical rating scale (NRS) where 0 is no pain or dull sensation and 10 is the strongest pain or dull sensation when the subjects' forearms with the weight (0.5 kg for women and 1 kg for men) were moved actively or passively to the full flexion and full extension positions. Blood flow in the deep tissues was evaluated based on the total hemoglobin (Hb) contents using near infrared spectroscopy (PSA-IIIN, Biomedical Science, Japan). Transverse ultrasound images of elbow flexors were obtained cautiously so as not to compress the tissues (SSA-340A, Toshiba, Japan). Distances from the surface of the humerus and from the skin to the outer surface of flexors were measured on the ultrasound image, and they were denoted as muscle and skin thickness, respectively.

Each measurement was evaluated by a different examiner. All subjects were asked to retrospectively draw a curve presenting the change in pain sensation (NRS) with each day for 1 week after exercise.

Vibration

Eight subjects received vibration at 30 Hz with amplitude of 8.0 mm shortly after all measurements were carried out following exercise (early-V group). Another 8 subjects received vibration after all measurements 2 days after exercise (late-V group). The vibrator (tip diameter 1.8 cm) was pressed on the belly and tendon of the biceps brachii muscle for 20 min in total with a strength that induced no apparent pain.

Data analysis

Data are expressed as mean ± SEM. One way analysis of variance (ANOVA) with repeated measures followed by Bonferroni's post hoc test was used to detect differences in the measures at different time points. The Kraskal-Wallis test was used for comparison among the three groups. Paired t-test was used for the effects of vibration to NRS in each group because NRS was 0 before exercise. Statistical significance was set at $p<0.05$.

The experiment was approved by the committee of Human Research, Research Institute of Environmental Medicine, Nagoya University.

Results

All subjects developed DOMS when examined 2 days after the exercise. Unexpectedly, the retrospective report of NRS with each day revealed that the highest soreness (NRS between 7.5 and 8.8) was experienced 1 day after the exercise, and NRS became lower 1 day later, between 5.4 and 5.5. Recovery from soreness was observed between 3 and 7 days after the exercise, and there were no significant differences in the magnitude of soreness and this time course among the three groups.

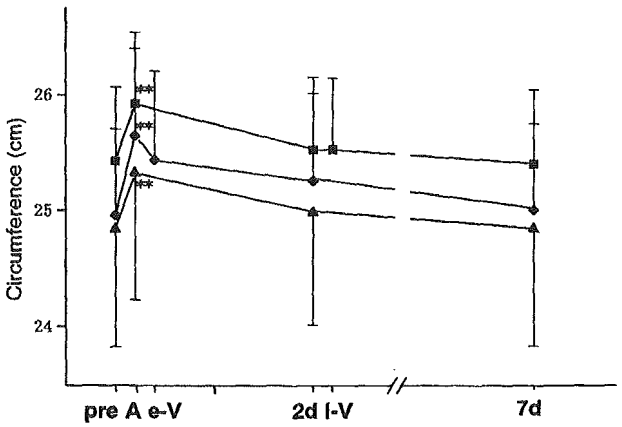

Fig. 1 Change in the circumference of the non-dominant arm. Ordinate: circumference in cm, Abscissa: time. pre: before exercise; **A**: immediately after exercise; **e-V**: immediately after vibration; **l-V**: after vibration 2 days after exercise; and **2d** and **7d**: 2 and 7 days after exercise. Rhombuses: early-V group; squares: late-V group; and triangles: control group. Values are shown as mean±SE. (** $p<0.01$, compared with the values before exercise, Bonferroni's multiple comparison test).

Circumference of the upper arm significantly increased in the two vibration groups after the exercise, but it returned to its original size 7 days after the exercise (Fig. 1). Vibration given either immediately or 2 days after the exercise had no effect on the arm circumference. The control group also showed a small increase in arm circumference, but it was not significant.

The elbow joint angle at maximum flexion decreased significantly after the exercise in all groups (Fig. 2). This angle before the exercise was 150.6 ± 1.8 degrees in the early-V group, 151.9 ± 0.9 degrees in the late-V group, and 150.8 ± 2.0 degrees in the control. After the exercise, it decreased to 74.4 ± 12.5, 83.8 ± 10.7, and 120.8 ± 6.9 degrees, respectively. **The elbow joint angle in maximum extension**, in contrast, tended to decrease immediately after the exercise but a significant decrease was observed only in the late-V group 2 days after the exercise. The vibration after exercise significantly increased these angles (ROM) ($p<0.01$). Two days after the exercise ROM was almost restored by vibration in the late-V group.

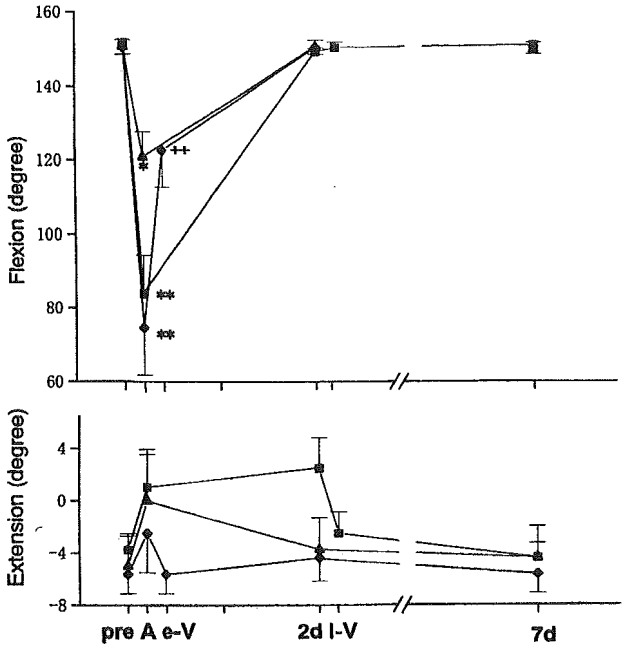

Fig. 2 Changes in the range of motion at elbow joint.
Upper panel shows the elbow angle in flexion and lower panel in extension. The presentation of abscissa is the same as in Fig. 1. The flexion range significantly decreased after exercise in all group (* $p<0.05$, ** $p<0.01$). The flexion range significantly increased after vibration in the early-V group (++ $p<0.01$).

Muscle soreness expressed in NRS in active movement, passive full flexion, and full extension peaked 2 days after the exercise (Fig. 3). Increased values of NRS in passive full flexion and extension were significantly decreased by vibration in the late-V group ($p<0.05$).

NRS of **dull sensation** in active movement and passive full flexion significantly increased after exercise in all groups. NRS of dull sensation in active movement was significantly decreased by vibration in the early-V group ($p<0.05$).

Blood flow in the deep tissues tended to decrease after the exercise in all groups, and it significantly increased after vibration in the early-V group ($p<0.01$).

Exercise did not affect the thickness of subcutaneous tissues that was measured using **ultrasound images**, whereas the thickness was significantly increased after vibration in both the early-V and late-V groups (Fig. 4, $p<0.01$ and $p<0.05$, respectively). In contrast, the thickness of flexor muscles of the upper arm became significantly thicker after exercise in all groups ($p<0.01$), and the thickness reduced again by the same amount 7 days after the exercise in all groups. In the early-V and late-V groups the thickness of flexors tended to reduce after vibration.

Subjects often complained of or reported pain when the exercised muscles were pressed with the vibrator or palpated with the fingers of the examiner. These complaints were less about 10 min after vibration started.

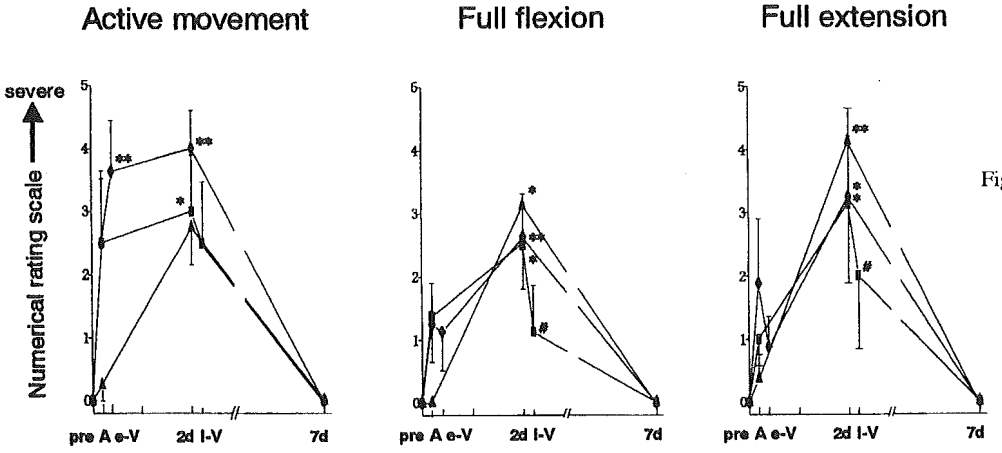

Fig. 3 Change in the soreness sensation of exercised muscle at three conditions. Ordinate: scale of 0 = no pain to 10 = intolerable pain. The presentation of abscissa is the same as in Fig. 1. Peak muscle pain was 2 days after exercise in all groups (* $p<0.05$, ** $p<0.01$). Peak muscle pain in full flexion and extension significantly decreased after vibration in the late-V group (# $p<0.05$, paired-t test).

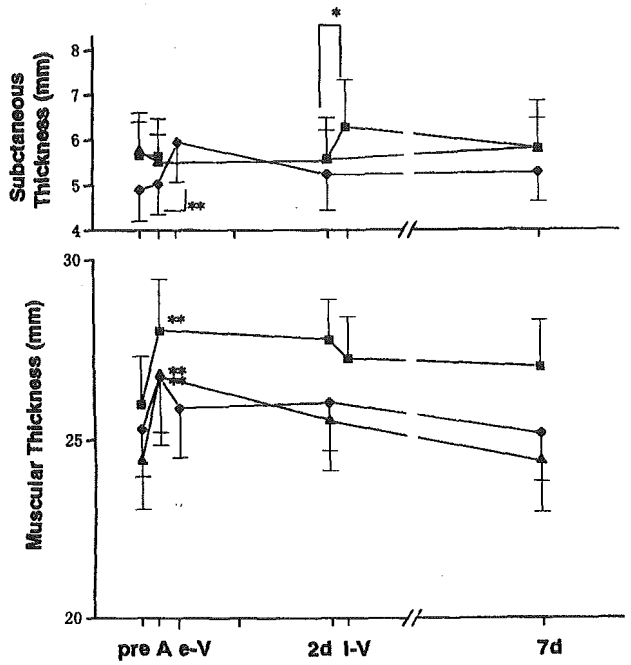

Fig. 4 Changes in the thickness of subcutaneous tissues and flexors. Upper panel: thickness of the subcutaneous tissues. Lower panel: thickness of the flexors. The thickness of flexors increased in all groups after exercise ($p<0.01$). The thickness of subcutaneous tissues was significantly increased after vibration in early-V and late-V groups (* $p<0.05$, ** $p<0.01$).

Discussion

The present study showed that DOMS was induced with the protocol used. Subjects' retrospective reports on soreness revealed that the peak soreness was experienced one day after exercise. Although soreness was not the strongest 2 days after the exercise, the circumference of the upper arm was larger, the extended elbow joint angle was limited and flexors were thicker. Also unexpected was the finding that, although all subjects of both sexes were randomly assigned to one of three groups, ROM was more strongly limited in both the early-V and late-V groups than in the control group, and soreness was also more intensive in these two groups. Subjects who regularly played sport were included in all groups, but they were not always less susceptible to DOMS. To obtain more conclusive results the number of subjects must be increased.

The circumference of the upper arm did not change after vibration in either the early-V or late-V group. This might be because the thickness of flexors decreased while the thickness of subcutaneous tissues increased after vibration.

It is clear that vibration improved ROM. The mechanism underlying the decrease in ROM has not been fully elucidated, but shortening of the connective tissue due to swelling and/or a spontaneous contraction of muscle fibers have been postulated (Clarkson, Nosaka et al. 1992). It has been demonstrated that a decrease of the maximally extended elbow joint angle is also related to increased muscle stiffness (Jones, Newham et al. 1987). It is known that vibration of muscle or tendon activates motoneurons through the tonic vibration reflex, simultaneously inhibiting the phasic myotatic reflexes that involve the motoneurons of the same pool. The Hoffman reflex is reported to be decreased with low frequency vibration (Desmedt and Godaux 1978). The decrease of muscle tone from vibration might have resulted in wider ROM.

Pain in active movement did not change after vibration in either of the vibration groups, but pain in the passively full-flexed and extended positions was reduced after vibration. Muscle tension generated during the active contraction with a weight is larger than that produced by passive movement. The vibration used in this study might have reduced the tension left in the previously exercised muscle, and thus have reduced the total muscular tension during passive flexion/extension below the pain threshold. However, if the tension was not strongly reduced, the total muscular tension during active contraction might have fallen below the pain threshold. For the moment it is not clear whether this is the case, but it would be reasonable to think that the difference in the total tension generated in the muscle during passive/active movement might be related with the difference in the effectiveness of vibration.

The thickness of subcutaneous tissues was significantly increased after vibration; in contrast, the thickness of the flexors tended to decrease after vibration, although this decrease was not significant. This result suggests that muscle swelling was reduced and subcutaneous edema was induced by vibration. Chleboun et al. (1998) reported that muscle stiffness increased immediately after exercise. This stiffness and hyperemia of the muscle are most likely related to muscle swelling. Since muscle tone is considered to be decreased by vibration (Desmedt and Godaux 1978), muscle stiffness and the thickness of flexors would also be decreased. On the other hand the mechanism of the thickening of subcutaneous tissues after vibration is not clearly understood. It might be caused by hyperemia because total Hb contained in the deep tissues increased during and after vibration. Again, the mechanism of this hyperemia is not clear.

In summary, vibration at 30 Hz widened ROM, decreased muscle soreness in full flexion and extension, increased the blood flow under the skin, exercised muscle and another connective tissues, increased the thickness of subcutaneous tissues, and tend to decrease the thickness of flexors. However, different from our clinical experience, these effects did not last long after vibration. This effect lasts a few days at least in the clinical setting. We usually apply vibration stimulation to the back muscles that belong to the same spinal segments as the sore muscles of the upper or lower limbs. Moreover the vibrator is pressed onto the muscle with a strength that induces pain. It may be necessary to use stronger vibration stimulation in the next experiment to produce more long-lasting effects. Moreover, clinical pain may be different from DOMS.

DOMS decreased in 3 and 7 days after exercise even if no treatment was done. Many clinical pains would not get better just by letting the time pass.

References

Armstrong RB, Warren GL, Warren JA. Mechanisms of exercise-induced muscle fibre injury. Sports Med 1991; 12: 184–207.

Chleboun GS, Howell JN, Conatser RR, Giesey JJ. Relationship between muscle swelling and stiffness after eccentric exercise. Med Sci Sports Exerc 1998; 30: 529–535.

Clarkson PM, Nosaka K, Braun B. Muscle function after exercise-induced muscle damage and rapid adaptation. Med Sci Sports Exerc 1992; 24: 512–520.

Desmedt JE, Godaux E. Mechanism of the vibration paradox: excitatory and inhibitory effects of tendon vibration on single soleus muscle motor units in man. J Physiol 1978; 285: 197–207.

Jones DA, Newham DJ, Clarkson PM. Skeletal muscle stiffness and pain following eccentric exercise of the elbow flexors. Pain 1987; 30: 233–242.

Nosaka K, Clarkson PM. Changes in indicators of inflammation after eccentric exercise of the elbow flexors. Med Sci Sports Exerc 1996; 28: 953–961.

Smith LL. Acute inflammation: the underlying mechanism in delayed onset muscle soreness?. Med Sci Sports Exerc 1991; 23: 542–551.

Received July 3, 2003; accepted July 22, 2003

Japanese Journal of Physiology, **52**, 521–530, 2002

Effects of Adrenoceptor Antagonists on the Cutaneous Blood Flow Increase Response to Sympathetic Nerve Stimulation in Rats with Persistent Inflammation

Tomoko KOEDA*,†, Jun SATO*, Takao KUMAZAWA‡, Yoichiro TSUJII†, and Kazue MIZUMURA*

* Department of Neural Regulation, Research Institute of Environmental Medicine, Nagoya University, Nagoya, 464–8601 Japan; † Department of Physical Therapy, School of Health Sciences, Nagoya University, Nagoya, 461–8673 Japan; and ‡ Emeritus Professor, Nagoya University, Nagoya, 464–8601 Japan

Abstract: There is some evidence that the sympathetic nervous system plays a role in the development and/or maintenance of painful states, and that sympathetic nervous function is altered in these conditions. Our previous experiments showed that electrical stimulation of the lumbar sympathetic trunk (sympathetic stimulation: SS), which normally induces a decrease in blood flow (BF) of plantar skin, induced its BF increase in about 50% of adjuvant-inflamed rats. To investigate the mechanism of this BF-increase response, we examined whether noradrenaline (NA) plays any role in this changed response to SS, and which receptor subtype is involved. We measured paw cutaneous BF response with a laser Doppler flowmeter in rats chronically inflamed with complete Freund's adjuvant. SS induced the BF-increase response in 50–67% of measured sites. Close-arterially injected NA induced the BF-increase response at dosages between 10–100 ng/kg only at the sites with the BF-increase response to SS. The BF-increase and -decrease responses to NA was significantly reduced after the close-arterial injection of either α1- or α2-adrenoceptor antagonists ($p<0.05$, respectively). In contrast, although the BF-decrease responses to SS were significantly reduced by administration of α1- and α2-adrenoceptor antagonist, BF-increase response was reduced only by α1-adrenoceptor antagonist, and that only at a higher dose. In addition, the β-adrenoceptor antagonist had no effects on both responses. These results suggest that the BF-increase response to SS involves, additionally to NA, a non-adrenergic mechanism. [Japanese Journal of Physiology, 52, 521–530, 2002]

Key words: sympathetic nerve stimulation, chronic inflammation, adrenoceptor, blood flow, rats.

Sympathectomy, or sympathetic ganglion blockade, has been shown to reduce pain in some chronic pain conditions such as complex regional pain syndrome (CRPS) [1–3]. Abnormalities of the skin temperature, coloring of the affected areas, and sweating have been observed in this condition [3]. These clinical findings suggest sympathetic nerve activity plays important roles in the development and/or maintenance of pain and accompanying changes of the affected tissues in these pathological conditions. Some efforts have been made to identify the mechanism of sympathetic involvement in pain, and α-adrenoceptor-mediated changes in nociceptive afferents, have been reported [4–7]. Some of these changes are common to inflamed conditions [7–10]: This would be plausible since recent studies suggest that CRPS has the distinct components of inflammation at its early stage [11]. On the other hand, sympathetic involvement in tissue changes has been less intensively investigated. Levine *et al.* [12] reported that sympathetic nerve activity affected

Received on July 17, 2002; accepted on October 17, 2002
Correspondence should be addressed to: Kazue Mizumura, Department of Neural Regulation, Research Institute of Environmental Medicine, Nagoya University, Furo-cho, Chikusa-ku, Nagoya, 464–8601 Japan. Tel: +81–52–789–3861, Fax: +81–52–789–3889, E-mail: mizu@riem.nagoya-u.ac.jp
Abbreviations: SS, electrical stimulation on the lumbar sympathetic trunk; BF, blood flow; NA, noradrenaline; CRPS, complex regional pain syndrome; CFA, complete Freund's adjuvant; AI, adjuvant-inflamed; MAP, mean arterial pressure; LST, lumbar sympathetic trunk; VC, vascular conductance; NO, nitric oxide; ATP, adenosine 5′-triphosphate; Ach, acetylcholine; PGs, prostaglandins; SP, substance P.

the degree of joint injury in the hind limb of experimentally arthritic rats. The vasoconstriction response to electrical stimulation of the sympathetic or saphenous nerve was diminished in a model of chronic inflammation induced by complete Freund's adjuvant (CFA) in rats [13, 14]. Lam and Ferrell also reported the vasoconstriction response to electrical stimulation of the sympathetic nerve was reduced in carrageenan inflammation rats [15]. Recently, it has been shown that chronic joint inflammation by CFA compromises α1- and α2-adrenoceptor function [16]. In our previous experiment investigating the involvement of sympathetic nervous activities in tissue changes in inflamed condition, we found that electrical stimulation of lumbar sympathetic nerve trunk (sympathetic stimulation: SS), which generally produces vasoconstriction of cutaneous blood vessels in normal animals, induced an increase in blood flow (BF) in the plantar skin of some adjuvant-inflamed (AI) rats [17]. The mechanism for this altered vascular response is not yet understood.

The aims of the present study, therefore, was to examine whether noradrenaline (NA), the major sympathetic nerve transmitter, plays any role in the altered vascular response, i.e., vasodilating response, to SS and which receptor subtypes are responsible for this effect. Before analyzing these points, we re-examined the distribution of the sites with increased BF in response to SS.

Preliminary accounts have appeared in abstract form [18–20].

METHODS

Induction of adjuvant inflammation. Fifty-eight male Lewis rats (LEW/Crj, Charles River Co., Yokohama, Japan) were used. They were 9 weeks old when CFA was injected. Adjuvant inflammation was induced in 53 rats by subcutaneously inoculating 0.1 ml of CFA, a suspension of heat-killed *Mycobacterium butyricum* (Difco Laboratories, Detroit, MI, USA) in paraffin oil (6 mg/ml), into the distal third of the tail. Five rats served as controls. All rats were kept on a 12-h light/dark cycle at 23°C with free access to food and water.

Surgery and lumbar sympathetic trunk stimulation. Rats that survived more than 2 weeks (maximum 11 weeks) after inoculation of the CFA were used for the experiment, since the symptoms of inflammation such as limping and redness of the feet appear about 2 weeks after the inoculation [21]. We did not find any difference in the response of the blood vessels between 2 and 11 weeks. Animals were initially anesthetized with α-chloralose and urethane (90 and 450 mg/kg I.P., respectively). The right jugular vein was cannulated for later administration of anesthetics. The animals spontaneously breathed the room air through a tracheal cannula. The right carotid artery was cannulated to measure mean arterial pressure (MAP). A branch of the femoral artery was cannulated for drug administration. Rectal temperature was maintained at 37.5±0.5°C using a heating pad and a lamp throughout the surgery and the recording period.

The lumbar sympathetic trunk (LST) was sectioned between L3 and L4 ganglia and communicating branches of spinal nerves in L4 ganglion were cut using a retroperitoneal approach under a binocular microscope, because sympathetic ganglia of L4 and below innervate the vascular bed of the surface of the hind paw [22]. An oil pool was made in the retroperitoneal cavity with skin flaps and the LST was kept in paraffin oil. The peripheral cut end of LST was placed on a bipolar platinum-stimulating electrode. The LST was stimulated by rectangular pulses of 0.2 ms duration and 10 V strength, at 1–5 Hz for 5 s. The frequency of the SS was adjusted so that the greatest vasodilating response was obtained; 5 Hz was the most frequently used frequency. The effects of SS were tested at intervals longer than 10 min. When supplemental anesthetic drug was added, a minimum of 10 min elapsed before the next SS. At the end of the experiments the rats were killed with an anesthetic overdose.

Laser Doppler flowmetry. The relative change in local BF was measured in the plantar skin of the right hind paw by a laser Doppler flowmeter (ALF21, Advance Co., Ltd., Tokyo, Japan). BF was simultaneously measured at two sites except a few antagonist-experiments. Electrical signals from the laser Doppler flowmeter and blood pressure monitor were simultaneously recorded and fed into a computer through an AD converter (DIGIDATA 1200, Axon Instruments, Inc., Foster City, CA, USA) using a data analysis program (AXOTAPE, Version 2.0, Axon Instruments, Inc.). The sampling intervals of the AD converter were 40 ms in the SS experiment and 100 ms with the administration of drugs. The sampled data were averaged every 1 s and expressed as arbitrary units for the BF and mmHg for the MAP. An apparent vascular conductance (VC) was calculated as the ratio of the BF to the MAP. However, we showed only the BF changes in the present results because the VC was similar to the BF. The BF, MAP, and VC values over 60 s before stimulation or drug administration were averaged and used as the baseline values. A change in the BF and MAP exceeding the baseline by

more than twice the standard deviation of the baseline value was used as the criterion for a response. To quantitatively analyze vascular changes, the difference between the baseline value and the maximum (or minimum) value after SS or injection of NA was calculated (as shown by ΔBF). We confirmed in every experiment that BF decreased to zero when rats were sacrificed.

Drug administration. NA (Sigma, St. Louis, MO, USA) and α-adrenergic antagonists were infused through a cannula inserted into a branch of the femoral artery by a microsyringe pump (EP-60, EICOM, Inc., Kyoto, Japan) with an infusion speed of 90 μl/min. A β-adrenoceptor antagonist, propranolol, was injected intravenously. NA was injected at dosages between 3 and 300 ng/kg up to a maximal BF-increase response was obtained. The effects of prazosin (Sigma), an α1-adrenoceptor antagonist, CH-38083, which is an α2-adrenoceptor antagonist having 400 times higher selectivity than yohinbine [23], and propranolol (Sigma), a β-adrenoceptor antagonist, were examined. Prazosin was dissolved in distilled water and another drugs were dissolved in saline and the infused volume was 30 μl. Saline was infused before and after administration of drugs without interruption since the BF was affected by the infusing fluid itself when the microsyringe pump was used.

Analysis. Results were expressed as the mean± SEM. The statistical significance was determined as follows: One way analysis of variance (ANOVA) with repeated measures followed by Bonferroni's test was used for comparison of the BF and MAP changes after drug administrations, and paired *t*-test for comparisons of the BF change after the injection of NA or SS in the presence as well as the absence of antagonists. Results were considered significant if $p<0.05$.

All experimental procedures were approved by the Animal Care Committee, Nagoya University.

RESULTS

The vasodilatation by SS in the AI rats

SS induced a decreased BF in the majority of normal rats, while it induced either an increase or a decrease of BF in the AI rats. Typical BF response to SS in the AI rats is shown in Fig. 1A. Two probes of the laser Doppler flowmeter were placed on the plantar skin in the case shown Fig. 1, and the BF responses to SS at these two sites were recorded simultaneously. A small (mean 4.6 mmHg, at 1 Hz), transient increase in MAP by SS was observed in 67.6% of the rats (a significant increase, $p<0.001$). The magnitude of SS-induced MAP-increase response was not different from that of control rats in preliminary experiment.

To determine whether there is any area with a preferential BF increase response, we trisected the plantar skin from the heel to the base of the toes and measured the BF at only one randomly selected site in each area. The BF responses in this series of experiments were successively examined in each trisected area. The frequency of the SS was fixed at 1 Hz in this experiment. SS decreased the BF in all sites except one in the control group (Table 1). In contrast, all ($n=12$) except one AI rat had BF-increase responses in more than one area measured. We found sites with a BF-increase response even in this exceptional rat

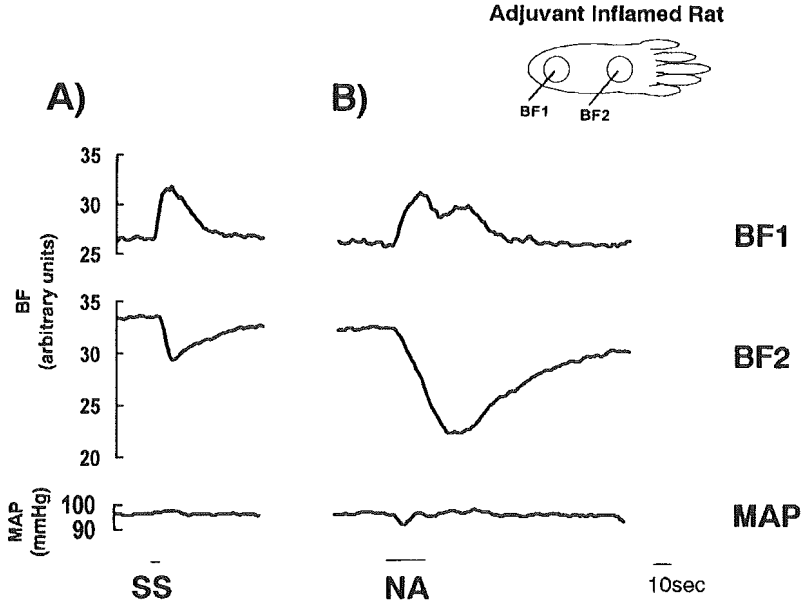

Fig. 1. Representative recordings of the blood flow (BF) and mean arterial pressure (MAP) responses to electrical stimulation of the lumbar sympathetic trunk (SS) and to injection of noradrenaline (NA) at different two sites in the same adjuvant-inflamed (AI) rat. A: The BF recordings obtained simultaneously at sites 1 and 2 (BF1, BF2: sites indicated in the schematic drawing of the hind paw) and MAP recording are shown. **B**: BF and MAP responses to NA injection at both site the same as in A. Bar indicates the period that SS (5 s) or NA injection at 100 ng/kg (20 s) was carried out. The scale for BF is shown at the upper left and for MAP is shown at the lower left. SS induced responses of both BF increase and decrease in the same rat. Where SS induced a BF-increase response, NA also induced a BF-increase response. MAP slightly increased to SS.

when we moved the probe to other sites within the respective areas. Thus, we found both BF-increase and -decrease responses in all AI rats, different from a previous report [17]. The ratio of randomly sampled sites exhibiting the BF increase response was 66.7% at the heel, 50.0% in the middle of the sole, and 58.3% at the base of the toes in the AI rats. There was no significant difference in these ratios among the three areas (χ^2 test, $p>0.05$).

Table 1. Effect of the sympathetic stimulation on the blood flow (BF). The plantar skin was divided to three areas, heel (A), middle (B), and the base of the toes (C). We measured BF response to SS at one randomly selected site in each area.

No.	A	B	C
Control			
1	−	−	+
2	−	−	−
3	−	−	−
4	−	−	−
5	−	−	−
Total	0/5	0/5	1/5
Adjuvant			
1	+	+	+
2	+	+	+
3	+	+	−
4	+	+	−
5	+	−	+
6	+	−	+
7	+	−	+
8	+	−	+
9	−	+	−
10	−	+	−
11	−	−	+
12	−	−	−
Total	8/12	6/12	7/12

+, BF increase response; −, BF decrease response. Each number shows one rat.

The following experiments were carried out in the AI rats only. When we simultaneously recorded BF at two sites, we firstly selected one site where the BF clearly increased in response to SS, and then we searched for a site where the BF decreased.

The BF response to NA

NA was close-arterially administered at doses between 3 and 300 ng/kg. The BF was increased when a lower dosage of NA was injected. Representative recordings of the BF responses to SS and NA injection (100 ng/kg) are shown in Fig. 1. Responses to SS and NA injection were similar at the same site, i.e., when SS induced BF increase, a small dosage of NA (Fig. 1B) did as well, and vice versa. Typical BF and MAP responses to different dosages of NA are shown in Fig. 2. NA with 3 ng/kg did not alter the BF. The BF-increase response was observed at between 30 and 100 ng/kg in the case shown in Fig. 2, and the response pattern to 30 ng/kg of NA was comparable with that to SS. At the same site, the BF increase became smaller with higher doses of NA (>100 ng/kg), suppressed by the developing BF decrease component. MAP was not changed at NA dosages that induced a BF increase only. In contrast, the magnitudes of the BF decrease at sites where BF decreased in response to SS increased unidirectionally with the concentration of NA, and the BF increase responses were never induced. The NA of doses between 10 and 100 ng/kg with some individual variations increased the BF (for criteria see the METHODS section) at sites with the BF-increase response to SS, and the BF de-

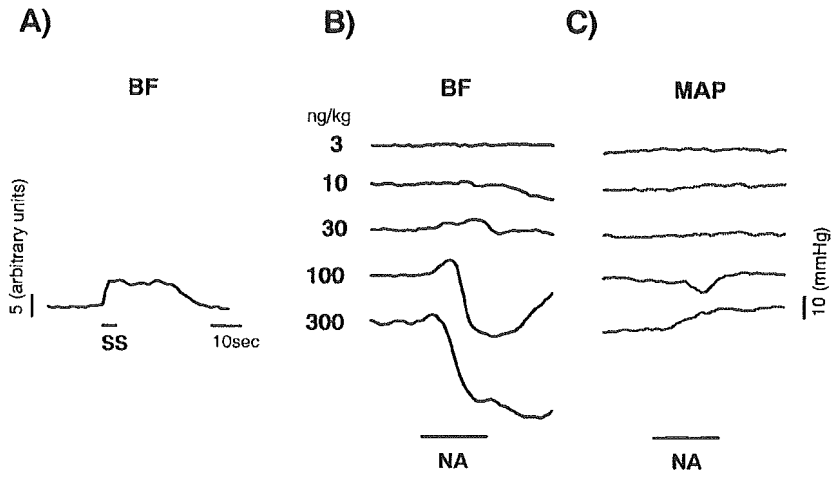

Fig. 2. Responses of the BF and MAP to different dosage of NA-a representative recording. A: BF increase response to SS. **B**: BF responses to NA injection. **C**: MAP responses to NA injection. The scale for BF is at the left and for MAP at the right. Bars indicate the period of SS (5 s) or injection of NA (20 s). NA was close-arterially administered at dosages between 3 and 300 ng/kg. BF was measured at the same site in an AI rat. Note that a BF increase was observed at dosages between 30 and 100 ng/kg, a BF decrease followed the BF increase at 100 ng/kg, and only the BF-decrease response was induced at 300 ng/kg (B). In this case, the BF response to NA of 30 ng/kg showed the same pattern as to SS. MAP was not changed by NA injection at any of the doses except 300 ng/kg (the MAP change by 100 ng/kg was not considered to be a drug effect because it was induced when the animal breathed deeply).

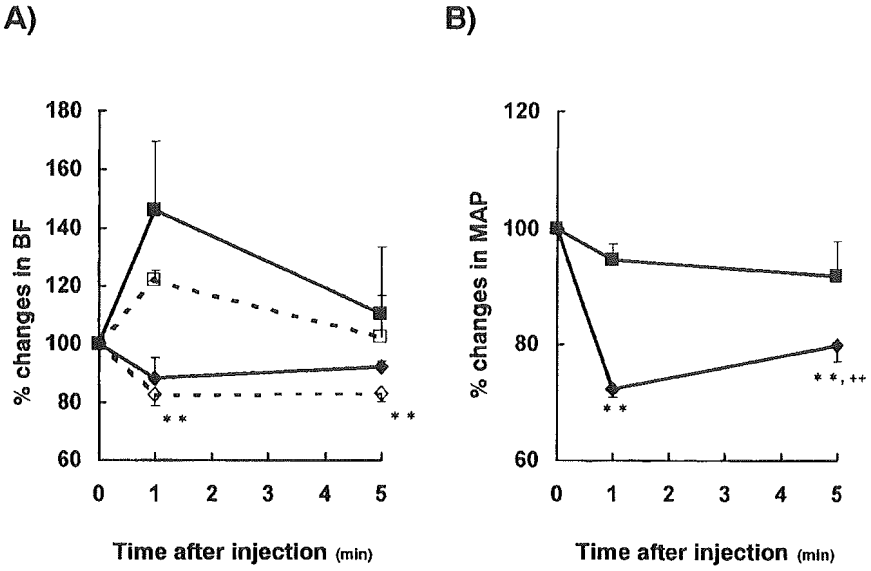

Fig. 3. Changes in basal BF and MAP induced by prazosin and CH-38083. A: Blood flow. Ordinate: % change in BF from the value before drug administration. Abscissa: time after injection. **B**: MAP. Ordinate: % change in MAP from the level before drug administration. Closed symbols and solid lines, measurement at the site of BF increase in response to SS in A; open symbols and dotted lines, measurement at the site of BF decrease in response to SS in A. Rhombus, prazosin (0.03 mg/kg); square, CH-38083 (0.3 mg/kg). Note that the BF at the BF-decrease site significantly decreased and at the same time MAP also significantly decreased after prazosin, suggesting that this change in the BF contains a passive component (**: $p<0.01$, respectively, $n=7$). ++: $p<0.01$ between 1 and 5 min after administration. CH-38083 tended to increase the BF, but the change was not significant.

crease followed at higher concentrations. These changes appear to be unaffected by repetitive injection of NA, as we did not observe any tachyphylaxis in preliminary experiments when we injected the same dosage of NA twice or three times with intervals of 10 min (data not shown).

Effects of α-adrenoceptor antagonists on BF responses to NA and SS

In the previous section we found that NA induced the BF increase in AI rats. However, this would not assure that NA mediated the SS-induced BF-increase response. Therefore, we examined the effects of two α-adrenoceptor antagonists on NA- and SS-induced BF responses and of a β-adrenoceptor antagonist on SS-induced BF-increase response in the AI rats. Prazosin (0.03 mg/kg, close-arterially injected) significantly decreased the baseline BF at the sites where BF decreased in response to SS, and thereafter the BF remained at this decreased level (Fig. 3, $p<0.01$). Prazosin did not significantly influence the baseline BF at the sites where the BF increased in response to SS. The MAP decreased significantly and then stabilized at a somewhat lowered level 5 min after injection of prazosin ($p<0.01$). This MAP change suggests that the observed BF decrease was mainly due to the decreased perfusion pressure, rather than that α1-adrenoceptor exerted a vasodilating action. The BF response to NA was examined when the BF and MAP reached this stable level. NA dosage was chosen for each rat that induced the maximal BF increase in the experiment described above. The BF increase in response to NA was significantly reduced by prazosin in 6 AI rats (Fig. 4A, B, $p<0.05$). The BF-decrease response to NA observed simultaneously but at a different site was also significantly reduced by prazosin in 6 AI rats (Fig. 4C, D, $p<0.05$).

When CH-38083 (0.3 mg/kg) was close-arterially injected, in contrast, the baseline BF value both at the sites where BF increased and decreased in response to SS tended to increase with considerable variation; however, these changes were not significant, and BF returned to the level previous to the antagonist injection in 5 min (Fig. 3A). The MAP was not changed by CH-38083 (Fig. 3B). This result suggests that α2-adrenoceptors were vasoconstrictory rather than vasodilatory both at the BF increase and decrease sites. The BF response to NA was examined when the BF reached a steady level. Both the BF increase and decrease responses to NA were significantly reduced at 8 min after the close-arterial injection of CH-38083 as well in 6 AI rats (Fig. 5, $p<0.05$).

The effects of adrenoceptor antagonists were different on the SS-induced BF-responses from the NA-induced BF-responses. Figure 6 shows a summary of the effects of prazosin (0.03 and 0.1 mg/kg, close-arterial injection) on the BF responses to SS. The BF-increase response to SS was significantly reduced by prazosin at higher dose (0.1 mg/kg, $p<0.05$, $n=5$) although prazosin at lower dose (0.03 mg/kg) did not affect the BF-increase response induced by SS ($p=0.12$, $n=8$). In contrast, the BF-decrease response to SS was significantly reduced by prazosin at both dosages (Fig. 6, $p<0.05$). MAP-increase response to SS was also

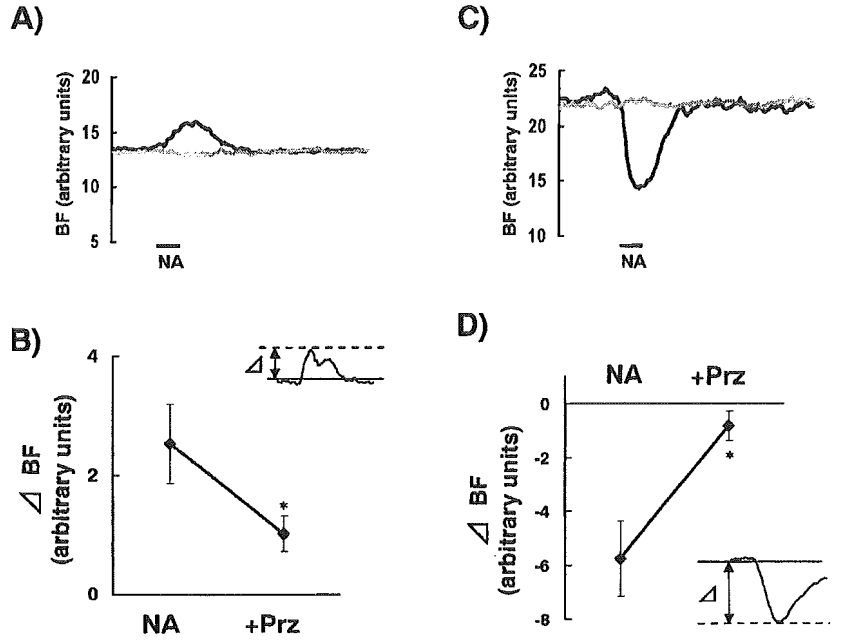

Fig. 4. Effects of prazosin, an α1-adrenorecepter antagonist, on the BF increase (A, B) and decrease (C, D) responses to NA. A, C: Sample recordings. Solid line, before administration of prazosin (0.03 mg/kg); dotted line, after administration of prazosin in the same AI rat. Ordinate: BF in arbitrary units. Bar: period of NA injection. B, D: Summary of the effect of prazosin. Ordinate: changes in the BF from baseline value (ΔBF). Either the maximum (BF-increase response) or the minimum (BF-decrease response) values after injection of NA were measured as shown in the **insets** and the mean values with SE were plotted (n=6). NA, NA response in the absence of prazosin; +Prz, NA response in the presence of prazosin. Prazosin significantly inhibited both the BF-increase and -decrease responses to NA (*: p<0.05, n=6, paired t-test).

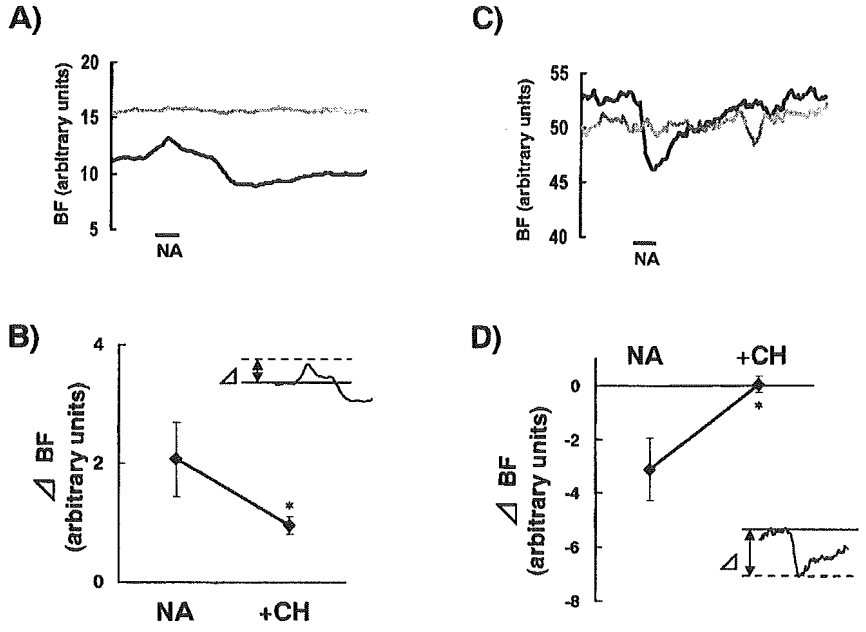

Fig. 5. Effects of CH-38083, an α2-adrenorecepter antagonist, on the BF-increase and -decrease responses to NA. The presentation is the same as in Fig. 4. CH-38083 (+CH) significantly inhibited both the BF-increase and -decrease responses to NA (*: p<0.05, n=6, paired t-test).

reduced by prazosin (p<0.05, n=7).

Effects of α2-adrenergic antagonist, CH38083, were also different from those on NA-induced BF changes. The BF-increase response induced by SS was not suppressed by close-arterial injection of CH-38083 at both 0.3 and 1 mg/kg (Fig. 7, p=0.45, n=5 and p=0.49, n=8, respectively). We failed to obtain any suppression of the BF-increase response to SS with CH-38083 at 10 mg/kg (in 2 AI rats, data not shown). In contrast the BF-decrease response induced by SS was significantly suppressed by close-arterial injection of CH-38083, though only at a higher dose (1 mg/kg, p<0.05, n=7). SS-induced MAP-increase was not affected by CH-38083 at 1 mg/kg (p=0.79, n=7).

Intravenously injected propranolol did not significantly modify the SS-induced BF-increase response (5.13±3.62 and 5.76±4.31 arbitrary unit before and after propranolol, respectively, p=0.42, n=5). Although MAP tended to increase after injection of propranolol, this effect was not statistically significant. SS-induced MAP-increase was not affected by propranolol at 1 mg/kg, either (p=0.62, n=5).

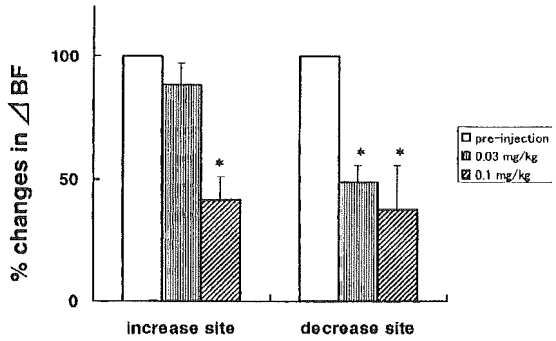

Fig. 6. Effects of prazosin at two different doses on the BF-increase and -decrease responses to SS. Ordinate: changes in BF (ΔBF) to SS were expressed as percentages of ΔBF before injection of prazosin. Abscissa: doses of prazosin at both SS-induced BF-increase and -decrease response sites. Striped column, 0.03 mg/kg; oblique hatched column, 0.1 mg/kg. The BF-increase response to SS was significantly reduced by prazosin at 0.1 mg/kg although 0.03 mg/kg had no effect (*: $p<0.05$). The BF-decrease response to SS was significantly inhibited by prazosin at 0.1 and 0.03 mg/kg (*: $p<0.05$).

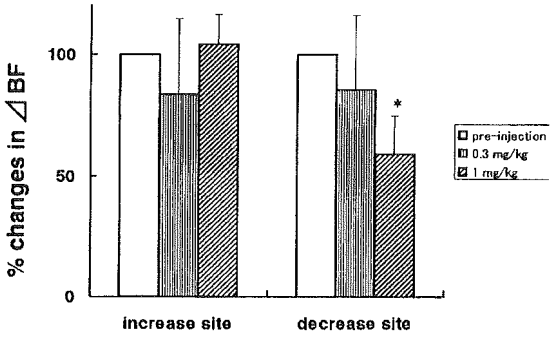

Fig. 7. The effects of CH-38083 at two different doses on the BF responses induced by SS. The presentation is the same as in Fig. 6. BF-increase response to SS was not significantly inhibited by CH-38083, whereas BF-decrease response to SS was significantly inhibited by CH-38083 at 1 mg/kg (*: $p<0.05$).

DISCUSSION

The BF increase response to SS was observed in all AI rats. We found in the present experiment that the BF increase response to SS was induced in all AI rats while it was rarely observed in control rats. In our previous study, the AI rats were classified into two groups [17], i.e., rats with a BF-increase response to SS and those with a BF-decrease response. We found both the BF-increase and -decrease responses simultaneously in the same AI rat as we moved the probe of the laser Doppler flowmeter. Sites of BF increase in response to SS were scattered all over the sole of the hind paw. The ratio of sites with the BF-increase response was 50–67% in each of the trisected areas of the plantar skin with random placement of the BF probe. This percentage was similar to the previous observation in that the BF increased in about half of the AI rats. The adjuvant-induced inflammation used in the present experiment is a generalized chronic condition characterized primarily by arthritis in the forepaw and hind paw, especially one or both hind paws. At times a mild diffuse pinkish swelling of the ankle and dorsal aspect of the tarsus was observed, and several localized lesions of the skin and mucous membrane were observed scattered over the whole body [24, 25]. Therefore, the scattering of the sites with the BF-increase response in the AI rats would seem to be related to the localized pathological changes.

The role of α-adrenoceptors in the BF response to SS. We found the lower dose of NA induced the BF-increase at the sites with the BF-increase response to SS, whereas the BF at the sites with the BF-decrease response to SS was decreased by NA irrespective of doses injected. We previously observed only BF-decrease response to NA, but only 400 ng/kg was used at that time [17]. We found in the present experiment that NA induced BF-increase at 10–100 ng/kg and BF-decrease followed at higher doses. This suggests NA is involved in the BF-increase response to SS in a limited condition.

The BF-increase responses to NA at a small dosage were reduced by either prazosin or CH-38083 (Figs. 4, 5). These results suggest that both α1- and α2-adrenoceptors mediated the BF-increase response to NA. The NA-induced BF-decrease response was also suppressed by both antagonists, suggesting mediation of both α1- and α2-adrenoceptors.

The BF-increase responses to NA observed in this experiment might have been active responses, i.e., active vasodilatation at the site where BF was measured, or a passive response resulting from redistribution of the BF after vasoconstriction in other areas. NA at dosage that induced BF-increase in this experiment did not influenced MAP, therefore, the redistribution of BF might be rather local. NA-induced vasodilatation, which is mediated through the α2-adrenoceptor, is known in larger vessels such as coronary and renal arteries [26], but this action was not found in smaller vessels such as those in which we measured BF in this experiment. The baseline values of the BF tended to increase, not decrease, at the sites with the BF-increase as well as at the sites with the BF-decrease response to SS when CH-38083 was administrated. These results suggest the α2-adrenoceptor did not dilate blood vessels under observation. Thus, the presently observed BF-increase response to NA might